ACS central science

Research Article

http://pubs.acs.org/journal/acscii

Transport Properties of Polysulfide Species in Lithium−Sulfur Battery Electrolytes: Coupling of Experiment and Theory

M. Safari,[†] C. Y. Kwok, and L. F. Nazar*

Department of Chemistry, University of Waterloo, 200 University Avenue West, Waterloo, Ontario N2L 3G1, Canada

Supporting Information

ABSTRACT: A comprehensive experimental and theoretical analysis of the isothermal transport of species for the two model ternary-electrolytes with LiTFSI-Li_2S_4/dioxolane (DOL)-dimethoxyethane (DME) and LiTFSI-Li_2S_6/DOL-DME formulations is presented. An unambiguous picture of the polysulfide's mobility is set forth after a detailed investigation of the macroscopic transference number and diffusion coefficients. The new findings of incongruent diffusion for Li_2S_4 species and high significance of cross-term diffusion coefficients reformulate a fledgling view of the prevalent redox-shuttle phenomena. The practical implications of this complex mechanism are discussed in detail.

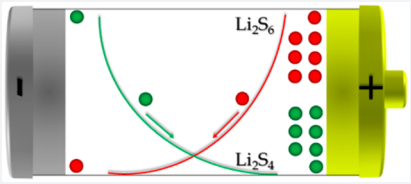

INTRODUCTION

Successful penetration of lithium−sulfur (Li−S) technology into the rechargeable battery market could serve the thirst for higher energy density battery systems in the electric-transport sector. These batteries that utilize lithium metal as the negative electrode and sulfur as positive electrode benefit from high theoretical specific capacity and energy density compared to lithium-ion batteries, coupled with low cost.[1−3] However, before their practical realization, there are many hurdles to overcome such as the insulating character of the active material end members (sulfur and Li_2S) on discharge and charge;[4] the corresponding large volume change;[5] lithium dendrite formation[6] during cell operation; and—most importantly—dissolution of the intermediate lithium polysulfide redox species into the electrolyte.[7] Unlike conventional Li-ion battery technologies, in a Li-sulfur battery, formation of a stable anode/electrolyte interface is mainly challenged by the intermediate species produced at the cathode. Understanding the underlying mechanisms of operation in Li−S cells especially remains a major obstacle to their continued improvement.[8] Extensive research is currently ongoing to minimize lithium polysulfide shuttles in Li−S batteries and to eliminate all its concomitant risks to the battery state of health. Much effort has been expanded in attempts to confine the soluble polysulfides via modification of cathode and cell design.[9−11] Some of these approaches include physical entrapment[12,13] or chemical adsorption[14,15] of polysulfides within the cathode network.

Moreover, electrochemical and operando spectroscopic studies reveal that the exact composition of these intermediates is solvent dependent and can be influenced by a series of chemical disproportionation reactions in the electrolyte.[16,17] Lu et al. used a rotating-ring disk electrode technique to probe the kinetics of the electrochemical reactions in Li−S cells,[18] while other researchers[19−21] focused more on the dominant soluble polysulfide species. These are effectively Li_2S_6 and Li_2S_4 in solvents of intermediate polarity such as dioxolane/dimethoxyethane (1:1 DOL/DME), which serves as the classical Li−S battery electrolyte, where lithium bis-trifluoromethane-sulfonimide (LiTFSI) is the conducting salt. Many studies show that Li_2S_8 is unstable toward disproportionation to these species, and Li_2S_2 is either unstable and/or insoluble.[20] In highly polar media such as dimethyl amide (DMA) and dimethyl sulfoxide (DMSO), the hexa-sulfide and tetra-sulfide dianions undergo cleavage to their monoanion radicals. In such media, $S_3^{-\bullet}$ the product of S_6^{-2} cleavage is especially prominent and is strongly favored in dilute solutions. This gives rise to the characteristic deep blue color of such solutions.[22,23] However, cleavage in DOL/DME is not favored at room temperature, and hence the concentration of the trisulfide radical is neglible.[24,25] Despite these many experimental studies to elucidate polysulfide speciation, very limited modeling work on Li−S batteries has been conducted that could provide an understanding of polysulfide transport properties, and hence their behavior in the cell. Only a few seminal and important studies have been reported,[7,26,27] contrary to lithium ion battery systems.[28−31] An accurate picture of species transport in the electrolyte is not only of fundamental importance, but is a prerequisite for any meaningful macroscopic modeling/optimization of the cell performance in a Li−S battery.[32−34] In this regard, experimental measure of a minimum number of the ion-transference numbers and diffusion coefficients for neutral combination of the ions, together with the ionic conductivity of the electrolyte is required.

Here, for the first time, we determine a complete set of transport properties for the binary electrolytes composed of Li_2S_6, Li_2S_4 (and the electrolyte salt, LiTFSI) dissolved in DOL/DME (1:1). These measurements are performed according to the original approach developed by Ma and Newman.[35] The theoretical/experimental frames provided by the thermodynamics of irreversible processes are further applied to estimate the transport properties for the more

Received: June 9, 2016
Published: July 28, 2016

DOI: 10.1021/acscentsci.6b00169
ACS Cent. Sci. 2016, 2, 560−568

practical ternary cases where the polysulfide and lithium salt are both present in the electrolyte.[36]

RESULTS

The restricted diffusion (RD), transference-polarization (TP), and concentration-cell (CC) experiments were all carried out on 1 mL of the electrolyte confined inside a Teflon (PFA) Swagelok cell. A schematic of this symmetric cell is presented in Figure 1 where a 12 mm PFA tube with an internal diameter of

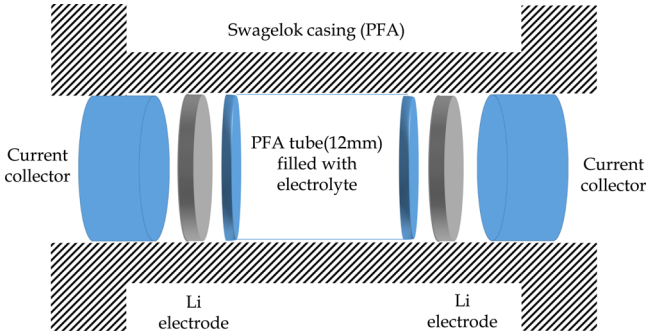

Figure 1. Schematic of the Swagelok cell used in this study for the electrochemical characterization of the electrolytes.

10 mm is positioned between the two lithium electrodes and filled with the electrolyte. In the concentration-cell (CC) experiments, the internal PFA tube is divided in two compartments separated with a 3 mm ultrafine porous glass frit to avoid mixing among the two compartments. The binary and ternary electrolytes with Li_2S_n (n = 6, 4) and LiTFSI as solutes were prepared in a 1,3 dioxolane/1,2 dimethoxyethane (DOL/DME) solvent (1−1 volume ratio) over a concentration range of 0.05−1.1 M in solute. Additional details are provided in Experimental Methods (see below).

Development of the Theoretical Framework. In a Li−S battery, the concentrated binary electrolyte (i.e., a primary lithium salt dissolved in a solvent) upon assembly turns into an electrolyte with a single cation (Li^+) and multiple anions (i.e., polysulfides in addition to the primary lithium-salt anion) over the course of battery operation.[20] Hence, in a Li−S battery and in the presence of n independent series of polysulfides, $\frac{(n+3)(n+2)}{2}$ transport properties are required to describe the isothermal transport of species in the electrolyte. This means that in the simplest case where only one of the high-order lithium-polysulfides (Li_2S_n, $4 \le n \le 8$) is dominant, one is left with a ternary electrolyte and six transport properties to be measured.

Here, our target is to provide consistent estimates of diffusion coefficients and transference numbers for a typical electrolyte used in Li−S cells. To do so, first, an appropriate formulation of species transport is presented for a general ternary electrolyte composed of a primary lithium salt, a single lithium-polysulfide (Li_2S_n), and a solvent. Further, the two approaches of Miller[37,38] and Ma et al.[35] are combined and adopted to the ternary electrolytes of LiTFSI and Li_2S_6 (Li_2S_4) dissolved in DOL/DME (namely, the binary coefficients were determined with the aid of three orthogonal experiments as set forth by Ma et al., and the ternary data are estimated according to Miller et al.).

Fundamental Transport Coefficients in a Ternary Electrolyte with a Common Cation. A ternary electrolyte with a common cation (C) and A1 and A2 as two anions can be represented as the following:

$$C_{\vartheta_{1,c}}A1_{\vartheta_{1,a}} \leftrightarrow \vartheta_{1,c}C^{z_1} + \vartheta_{1,a}A1^{z_2} \quad (1)$$

$$C_{\vartheta_{2,c}}A2_{\vartheta_{2,a}} \leftrightarrow \vartheta_{2,c}C^{z_1} + \vartheta_{2,a}A2^{z_3} \quad (2)$$

where, $\vartheta_{i,c}$ and $\vartheta_{i,a}$ are the stoichiometries of the cation and anions in the ith solute (i = 1, 2), and the charge numbers of the common cation and two anions are represented by z_1, z_2, and z_3, respectively. Isothermal transport of species in such a system is described by two independent transference numbers, four diffusion coefficients for neutral combinations of ions (out of which three are independent) and the ionic conductivity of the electrolyte. These measurable macroscopic properties are expressed with the aid of nine fundamental transport coefficients (l) where only six are independent according to the Onsager reciprocal relations.[36] In a solvent-fixed frame (SF), hereafter represented by 0 in the superscript, the flux equations for the ions (i.e., J_C^0, J_{A1}^0, J_{A2}^0) in one dimension are

$$J_C^0 = J_1^0 = \frac{t_1^0}{Fz_1}I - (\vartheta_{1,c}\mathcal{D}_{22}^0 + \vartheta_{2,c}\mathcal{D}_{32}^0)\nabla\mu_{12} - (\vartheta_{1,c}\mathcal{D}_{23}^0 + \vartheta_{2,c}\mathcal{D}_{33}^0)\nabla\mu_{13} \quad (3)$$

$$J_{A1}^0 = J_2^0 = \frac{t_2^0}{Fz_2}I - \vartheta_{1,a}\mathcal{D}_{22}^0\nabla\mu_{12} - \vartheta_{1,a}\mathcal{D}_{23}^0\nabla\mu_{13} \quad (4)$$

$$J_{A2}^0 = J_3^0 = \frac{t_3^0}{Fz_3}I - \vartheta_{2,a}\mathcal{D}_{32}^0\nabla\mu_{12} - \vartheta_{2,a}\mathcal{D}_{33}^0\nabla\mu_{13} \quad (5)$$

where I is the total current density and F is the Faraday constant. In these flux equations, $\nabla\mu_{12}$ and $\nabla\mu_{13}$ are the electrochemical potential gradients of the neutral combination of the common cation (denoted as subscript 1) with the first (2) and second (3) anions, respectively, and are related to their concentration counterparts (i.e., ∇c_{12}, ∇c_{13}) according to the following equation:[39]

$$\nabla\mu_{1i} = RT\left[(\vartheta_{i-1,c} + \vartheta_{i-1,a})\frac{\partial \ln f_{\pm}^{1i}}{\partial c_{12}} + \frac{\vartheta_{1,c}\vartheta_{i-1,c}}{\vartheta_{1,c}c_{12} + \vartheta_{2,c}c_{13}} + \frac{\vartheta_{i-1,a}}{c_{1i}}\delta_{1,i-1}\right]\nabla c_{12} + RT\left[(\vartheta_{i-1,c} + \vartheta_{i-1,a})\frac{\partial \ln f_{\pm}^{1i}}{\partial c_{13}} + \frac{\vartheta_{2,c}\vartheta_{i-1,c}}{\vartheta_{1,c}c_{12} + \vartheta_{2,c}c_{13}} + \frac{\vartheta_{i-1,a}}{c_{1i}}\delta_{2,i-1}\right]\nabla c_{13},\ (i = 2, 3) \quad (6)$$

where δ is the Kronecker delta function, R is the universal gas constant, and T is temperature. The molar concentrations and mean-molar ionic activity coefficients of the two solutes (i.e., $C_{\vartheta_{1,c}}A1_{\vartheta_{1,a}}$ and $C_{\vartheta_{2,c}}A2_{\vartheta_{2,a}}$) are represented by ($c_{12}$, c_{13}) and ($f_{\pm}^{12}$, $f_{\pm}^{13}$), respectively.

The transference numbers (t^0) and fundamental diffusion coefficients ($\mathcal{D}^0$) are expressed with the aid of more fundamental transport coefficients (l^0) set forth by the thermodynamics of irreversible processes according to eqs 7 and 8, respectively.[36−38]

$$t_i^0 = \frac{F^2 z_i \sum_{k=1}^{k=3} z_k l_{ik}^0}{\kappa},\ i = 1, 2, 3 \quad (7)$$

DOI: 10.1021/acscentsci.6b00169
ACS Cent. Sci. 2016, 2, 560−568

$$\mathcal{D}^0_{ij} = \frac{F^2}{\kappa}\sum_{k=1}^{3}\sum_{w=1}^{3}\frac{z_k z_w}{\vartheta_{i-1,a}\vartheta_{j-1,a}}(l^0_{ij}l^0_{kw} - l^0_{iw}l^0_{kj}),\ i, j = 2, 3 \tag{8}$$

where, in eq 7 and 8, κ is the electrolyte conductivity:

$$\kappa = F^2\sum_{k=1}^{3}\sum_{w=1}^{3} z_k z_w l^0_{kw} \tag{9}$$

However, the transference numbers and diffusion coefficients are dependent on the chosen frame of reference. Transference numbers are experimentally measured in a solvent-fixed (SF) frame, whereas the practical diffusion coefficients are usually measured in a volume-fixed frame of reference (VF). Practical diffusion coefficients (D) and fundamental ones ($\mathcal{D}$) are related according to eq 10

$$\sum_{j=2}^{3} D_{ij}\nabla c_{1j} = \sum_{j=2}^{3}\mathcal{D}_{ij}\nabla\mu_{1j},\ i = 2, 3 \tag{10}$$

It is more convenient to set forth the transport equations in SF and further use the following equation to transform the practical diffusion coefficients between the two frames of reference (i.e., SF and VF):[40]

$$D^{v}_{ij} = \sum_{k=2}^{3}(\delta_{ki} - c_{1i}\overline{V}_{1k})D^0_{kj},\ i, j = 2, 3 \tag{11}$$

where $\overline{V}_{12}$ and $\overline{V}_{13}$ are the partial molar-volumes of $C_{\vartheta 1,c}A1_{\vartheta 1,a}$ and $C_{\vartheta 2,c}A2_{\vartheta 2,a}$, respectively, and are experimentally measured with the aid of the following equation:[41]

$$\overline{V}_{1i} = \frac{M_{1i} - \frac{\partial\rho}{\partial c_{1i}}}{\rho - \sum_{j=2}^{3} c_{1j}\frac{\partial\rho}{\partial c_{1j}}},\ i = 2, 3 \tag{12}$$

where M_{12} and M_{13} are the molar masses of $C_{\vartheta 1,c}A1_{\vartheta 1,a}$ and $C_{\vartheta 2,c}A2_{\vartheta 2,a}$, respectively, and ρ is the density of the ternary electrolyte.

Note that in Miller's original treatment of ternary electrolytes with a common anion,[38] he distinguished between the chemical and electrical potentials in the entropy production term. This separation is unnecessary,[39] though similar results are obtained when the thermodynamic force is defined in terms of the electrochemical potentials.

Estimation of Ternary Transport Properties from Experimental Binary Data. The six fundamental transport coefficients (l^0_{ij}) for the system defined by eqs 1 and 2 are estimated based on the measured coefficients ($l^{0,b}_{ij}$) for the two isolated binary systems, defined by eqs 1 and 2, and application of the following correlations after Miller:[38]

$$l^0_{ii} = x_{1i}(l^{0,b}_{--})_{1i,N},\ i = 2, 3 \tag{13}$$

$$l^0_{11} = x_{12}(l^{0,b}_{++})_{12,N} + x_{13}(l^{0,b}_{++})_{13,N} \tag{14}$$

$$l^0_{1i} = x_{1i}(l^{0,b}_{+-})_{1i,N},\ i = 2, 3 \tag{15}$$

$$l^0_{23} = x_{12}x_{13}(l^0_{12}l^0_{13})^{0.5} \tag{16}$$

where $l^{0,b}_{+-}$, $l^{0,b}_{++}$, and $l^{0,b}_{--}$ are the cation−anion, cation−cation, and anion−anion interaction coefficients in the binary electrolytes, respectively. These binary coefficients are evaluated at a total (N) number of equivalents in the ternary electrolyte:

$$N = |\vartheta_{1,a}z_2c_{12} + \vartheta_{2,a}z_3c_{13}| = z_1(\vartheta_{1,c}c_{12} + \vartheta_{2,c}c_{13}) \tag{17}$$

In eqs 13−16, x_{12} and x_{13} are the equivalent fractions and are defined as the following:

$$x_{1i} = \frac{N_{1i}}{N},\ i = 2, 3 \tag{18}$$

$$N_{1i} = |\vartheta_{i-1,a}z_ic_{1i}|,\ i = 2, 3 \tag{19}$$

Transference numbers, conductivity, and fundamental diffusion coefficients ($\mathcal{D}^0_{ij}$) for the ternary system (eqs 1 and 2) are readily available (eqs 7−9) after estimation of l^0_{ij}. Derivatives of mean-molar ionic activity coefficients ($f^{12}_{\pm}$ and $f^{13}_{\pm}$) are required, however, in order to obtain practical diffusion coefficients (D^0_{ij}). Providing that these thermodynamic parameters are known for the binary constituents ($f^{12,b}_{\pm}$ and $f^{13,b}_{\pm}$), the Scatchard's neutral-electrolyte description can be used to estimate $f^{12}_{\pm}$ and $f^{13}_{\pm}$ in the ternary system:[42]

$$\frac{\ln f^{1i}_{\pm}}{z_1z_i} = \frac{1}{2}\frac{\ln f^{1i,b}_{\pm}}{z_1z_i} + \frac{1}{2}\left[y_{12}\frac{\ln f^{12,b}_{\pm}}{z_1z_2} + y_{13}\frac{\ln f^{13,b}_{\pm}}{z_1z_3}\right] + \beta_i,\quad i = 2, 3 \tag{20}$$

$$\beta_i = \frac{1}{2}\left[\frac{y_{12} + \delta_{i2}}{z_1z_2}\ln\frac{(c^b_0)_{12}M_0}{\rho_0} + \frac{y_{13} + \delta_{i3}}{z_1z_3}\ln\frac{(c^b_0)_{13}M_0}{\rho_0}\right] - \frac{1}{z_1z_i}\ln\frac{c_0M_0}{\rho_0},\ i = 2, 3 \tag{21}$$

where c_0 and $(c^b_0)_{1i}$ are the solvent concentrations in the ternary and binary electrolytes, respectively, ρ_0 is the solvent density, and M_0 is molar mass of the solvent. In eqs 20 and 21, all the binary parameters are evaluated at the total ionic-strength of the ternary electrolyte and y defines the ionic-strength fraction[42] of each solute in the ternary electrolyte according to

$$y_{1i} = \frac{c_{1i}\vartheta_{i-1,c}z_1(z_1 - z_i)}{\sum_{j=2}^{3} c_{1j}\vartheta_{j-1,c}z_1(z_1 - z_j)},\ i = 2, 3 \tag{22}$$

Fundamental Transport Coefficients for the Binary Electrolytes of LiTFSI and Li_2S_n (n = 6, 4) in DOL/DME. Here, we are interested at experimental measure of $l^{0,b}_{+-}$, $l^{0,b}_{++}$, and $l^{0,b}_{--}$ for the three binary systems described by eqs 23−25

$$\text{Li TFSI} \leftrightarrow \text{Li}^{+1} + \text{TFSI}^{-1},\ \text{(solvent: DOL/DME)} \tag{23}$$

$$\text{Li}_2\text{S}_6 \leftrightarrow 2\text{Li}^{+1} + \text{S}_6^{-2},\ \text{(solvent: DOL/DME)} \tag{24}$$

$$\text{Li}_2\text{S}_4 \leftrightarrow 2\text{Li}^{+1} + \text{S}_4^{-2},\ \text{(solvent: DOL/DME)} \tag{25}$$

It is straightforward to show that in a binary electrolyte, the three fundamental transport coefficients can be expressed as a function of three macroscopic and measurable transport properties (i.e., κ^b, $t^{0,b}_i$, and $D^{V,b}$) in eq 26

$$l^{0,b}_{ij} = \frac{\kappa^b t^{0,b}_i t^{0,b}_j}{F^2 z_iz_j} + (-1)^{\delta_{ij}}\frac{\vartheta_+\vartheta_-z_+z_-c^bD^{V,b}}{RTz_iz_j(\vartheta_+ + \vartheta_-)\left(1 + \frac{\partial\ln f^b_{\pm}}{\partial\ln c^b}\right)c_0{}^b\overline{V}_0{}^b},\ i, j = +, - \tag{26}$$

DOI: 10.1021/acscentsci.6b00169
ACS Cent. Sci. 2016, 2, 560−568

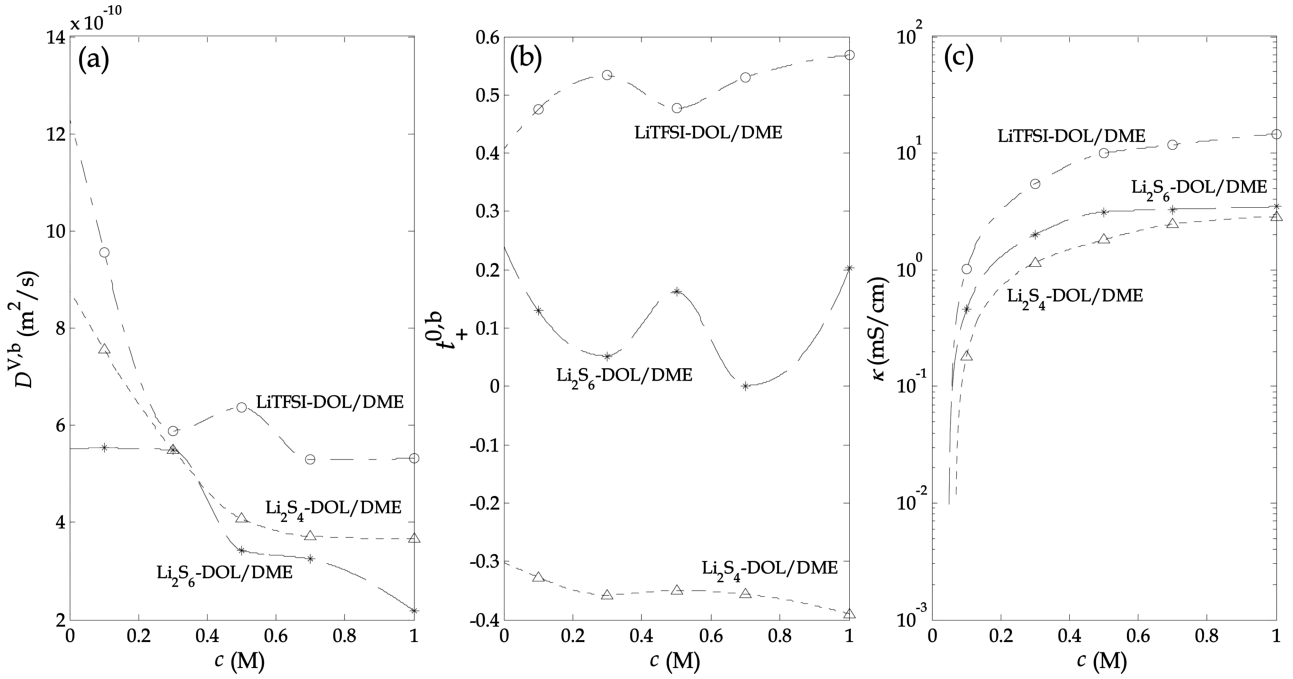

Figure 2. Transport coefficients: (a) practical diffusion coefficient in a volume-fixed frame of reference, (b) transference number of lithium ions in a solvent-fixed frame of reference (c) electrolyte ionic conductivity—in the binary electrolytes of LiTFSI-DOL/DME (dash-dot-○-), Li_2S_4-DOL/DME (dot-△-), and Li_2S_6-DOL/DME (dash-*-) at T = 25 °C. Markers are experimental data and lines are shape-preserving fits only for improved visualization.

where $\bar{V}_0{}^b$ and $c_0{}^b$ are the partial molar-volume and concentration of the solvent, respectively, and c^b is the solute concentration in the binary electrolyte.

The value κ^b is readily attained with the application of AC-impedance spectroscopy. The high frequency intercept on the x (real)-axis in a Nyquist plot is a sufficiently accurate measure of the ohmic resistance of the electrolyte. This resistance, together with the known geometry of the cell, provides us with the specific ionic conductivity of the electrolyte which is independent of the frame of reference used during the measurement. However, the experimental measurement of $t_i^{0,b}$ and $D^{V,b}$ is not trivial. In the following, the elegant approach originally developed by Ma et al.[35] and lately improved by Hafezi and Newman[43] is applied to the case of binary electrolytes investigated in this study (eqs 23−25). Here, and for the sake of simplicity, the solvent system (DOL/DME) is treated as a single component. The transference number of lithium ions ($t_+^{0,b}$) and the mean-molar ionic activity coefficient of the solutes ($f_\pm^b$) are coupled together according to eq 27 in the absence of current ($I = 0$)[41]

$$\nabla\Phi = \frac{(\vartheta_+ + \vartheta_-)RT}{\vartheta_+ z_+ F}\left(1 + \frac{\partial \ln f_\pm^b}{\partial \ln c^b}\right)(1 - t_+^{0,b})\nabla \ln c^b \tag{27}$$

where Φ is a well-defined potential in the electrolyte with respect to a lithium reference electrode.

Application of eq 27 to the results from a series of concentration-cell experiments provides one with the product of thermodynamic factor $\left(1 + \frac{\partial \ln f_\pm^b}{\partial \ln c^b}\right)$ and the transference number of the anion (i.e., $1 - t_+^{0,b}$). In the concentration-cell experiments, the potential difference is recorded ($I = 0$) between the two lithium electrodes ($\Delta\Phi$) in a cell filled with different concentrations of a given solute at the left (c_l^b) and right (c_r^b) compartments. Transference-polarization (TP) tests are performed to compensate for the dearth of data regarding the thermodynamic factor of the solute (which could be obtained independently via vapor pressure or isopiestic measurements with great effort). In TP experiments, a short pulse of current is applied to an equilibrated symmetric cell made of the lithium electrodes and the binary electrolyte under study at a given initial concentration (c_∞^b). The difference of solute concentration (Δc^b) between the vicinity of the two electrodes created by the current pulse is[43]

$$\Delta c^b = \frac{4(1 - t_+^{0,b})I}{F\vartheta_+ z_+ D_\infty^{V,b}}\sqrt{\frac{D_\infty^{V,b} t_p}{\pi}}\,\tau \tag{28}$$

where t_p is the pulse duration and $D_\infty^{V,b}$ is the diffusion coefficient of solute in the electrolyte at $c^b = c_\infty^b$ and in VF. τ is a dimensionless time and is defined by eq 29:

$$\tau = \frac{\sqrt{t_p}}{\sqrt{t} + \sqrt{t - t_p}} \tag{29}$$

In eq 29, t is the time elapsed from the beginning of the TP experiment and extends to the relaxation period to the point where the cell retrieves its equilibrium ($\Delta c^b = 0$). During the TP experiment, this is the potential across the cell and not the concentration difference which is recorded. For sufficiently small perturbations ($I\sqrt{t_p} \to 0$), Δc^b can be evaluated from eq 30:

$$\Delta c^b = \frac{\Delta\Phi c_\infty^b}{\left(\frac{d(\Delta\Phi)}{d \ln c^b}\right)_{CC, c_\infty^b}} \tag{30}$$

DOI: 10.1021/acscentsci.6b00169
ACS Cent. Sci. 2016, 2, 560−568

Table 1. Calculated Partial Molar Volumes of Solvent (i.e., DOL/DME) and Solutes in the Binary and Ternary Mixtures of Li_2S_4, Li_2S_6, and LiTFSI[a]

	component				
solution	$\bar{V}_{Li_2S_4}$ (cm^3/mol)	$\bar{V}_{Li_2S_6}$ (cm^3/mol)	$\bar{V}_{LiTFSI}$ (cm^3/mol)	$\bar{V}_{DOL/DME}$ (cm^3/mol)	solution density (g/cm^3)
DOL/DME-Li_2S_4	44			84	$\rho = 0.0996c_{13} + 0.9647$
DOL/DME-Li_2S_6		65		84	$\rho = 0.1438c_{13} + 0.9638$
DOL/DME-LiTFSI			134	83	$\rho = 0.157c_{12} + 0.968$
DOL/DME-Li_2S_4–LiTFSI	38		128	84	$\rho = 0.1076c_{13} + 0.1638c_{12} + 0.9644$
DOL/DME-Li_2S_6–LiTFSI		75	125	83	$\rho = 0.1336c_{13} + 0.1656c_{12} + 0.9689$

[a]Calculations are based on the solution densities measured at 25 °C. Individual solute concentrations are between 0.1 and 1 M.

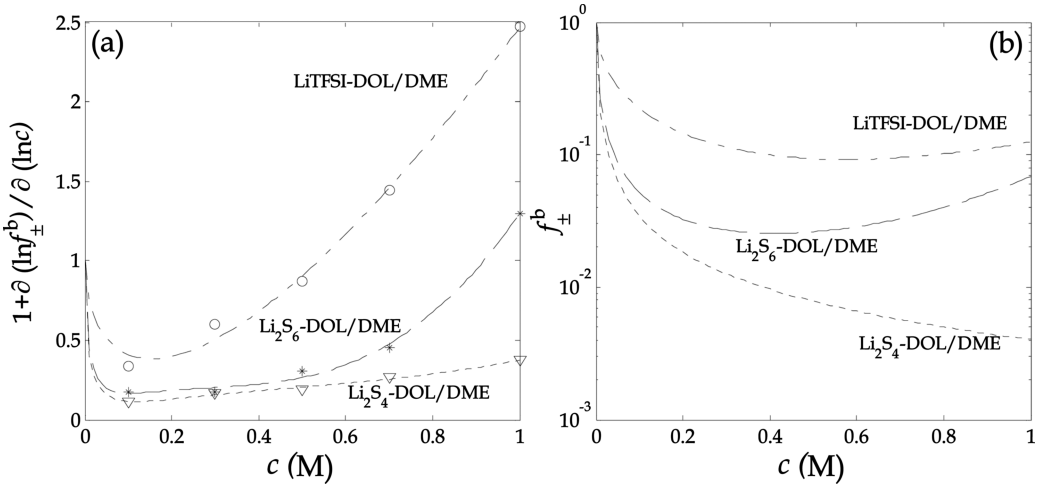

Figure 3. (a) Thermodynamic factor and (b) mean-molar ionic activity coefficients of solutes in the binary electrolytes of LiTFSI-DOL/DME (dash-dot-○-), Li_2S_4-DOL/DME (dot-△-), and Li_2S_6-DOL/DME (dash-*-) at T = 25 °C. Markers are experimental data and lines represent the empirical fits or processed data.

where the denominator on the right-hand side of the equality is the slope of a $\Delta\Phi-\ln c^b$ plot evaluated at $c^b = c^b_\infty$ and is accessible through the data analysis of the concentration-cell experiments. Accordingly, combination of eqs 28 and 30 results in the following correlation between $\Delta\Phi$ and τ in TP experiments

$$\Delta\Phi = \left[\left(\frac{d(\Delta\Phi)}{d\ln c^b}\right)_{CC,c^b_\infty} \frac{4(1-t_+^{0,b})}{F\vartheta_+ z_+ c^b_\infty D^{V,b}_\infty}\sqrt{\frac{D^{V,b}_\infty}{\pi}} I\sqrt{t_p}\right]\tau \quad (31)$$

The slope of $\Delta\Phi-\tau$ plots are calculated for a series of TP tests with different values of $I\sqrt{t_p}$. The quantity inside the bracket in eq 31 is then plotted against $I\sqrt{t_p}$ and the resulting slope represented by m is used for unequivocal resolution of transference number:

$$t_+^{0,b} = 1 - \frac{F\vartheta_+ z_+ c^b_\infty \sqrt{\pi D^{V,b}_\infty}}{4\left(\frac{d(\Delta\Phi)}{d\ln c^b}\right)_{CC,c^b_\infty}} m \quad (32)$$

An a priori knowledge of $D^{V,b}_\infty$ enables us to calculate both the thermodynamic factor and the transference number at the same concentration of solute by the application of eq 27 and eq 32, respectively. Here, $D^{V,b}_\infty$ is obtained with the application of the method of the restricted diffusion (RD) to a similar cell used in TP experiment.[44] Contrary to the TP experiment where t_p is in the order of few minutes, in RD, the cell is held under polarization for a very long time (i.e., few hours). The natural logarithm of the potential relaxation is plotted against time of which a linear trend is found toward equilibrium. The slope of the linear tail (s_D) is related to $D^{V,b}_\infty$ according to eq 33

$$-s_D = \frac{\pi^2}{L^2} D^{V,b}_\infty \quad (33)$$

where L is the distance between the two electrodes.

DISCUSSION

It is important to note that the application of eqs 27–33 for the case of polysulfide systems (eqs 24 and 25) is subject to two main assumptions. First, any disproportionation reactions cannot be explicitly accounted for owing to the complexity involved (and lack of experimental data on their kinetics), and second, the flux of polysulfide anions (i.e., S_4^{-2} and S_6^{-2}) is taken to be zero at both electrodes. A more comprehensive analysis would be possible only with *a priori* access to the kinetic parameters of the polysulfides in the disproportionation and side reactions at the bulk of electrolyte and surface of the lithium electrode, respectively. We believe these are both reasonable assumptions. Under dilute conditions, and in a solvent of intermediate polarity such as DOL/DME, disproportionation reactions at static Li/S ratios as used here are not expected to be high.[45]

The macroscopic transport coefficients for the three binary electrolyte systems (i.e., eqs 23–25) at 25 °C and for solute concentrations in the range of 0.1–1 M are presented in Figure 2a–c. The diffusion coefficient of the lithium salt and lithium polysulfides features a decreasing trend upon the concentration increase, and the average $D^{V,b}$ is the same order of magnitude

DOI: 10.1021/acscentsci.6b00169
ACS Cent. Sci. 2016, 2, 560–568

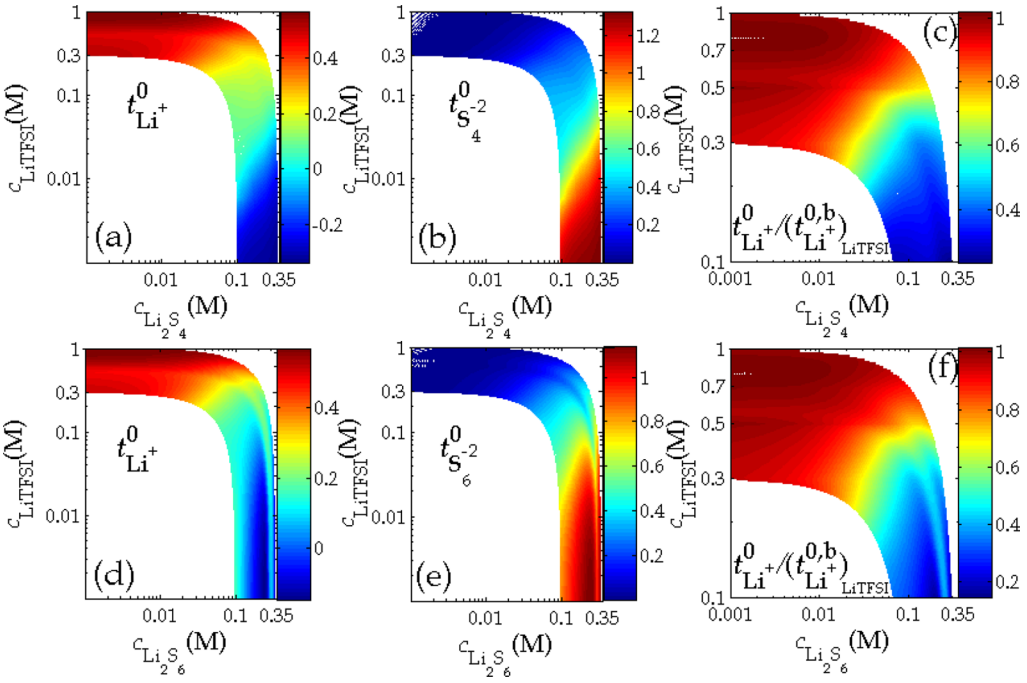

Figure 4. Lithium transference numbers at T = 25 °C, in the ternary electrolytes (a) LiTFSI-Li_2S_4 and (d) LiTFSI-Li_2S_6 and their ratio with respect to the corresponding values in a binary electrolyte of LiTFSI at the same concentration of LiTFSI as in those of ternary (c) LiTFSI-Li_2S_4 and (f) and LiTFSI-Li_2S_6. Polysulfide transference numbers in the ternary electrolytes of (b) LiTFSI-Li_2S_4 and (e) LiTFSI-Li_2S_6.

$(3.5 \times 10^{-10} < (D^{V,b})_{ave} < 6.5 \times 10^{-10}$ m^2/s) for the three solutes (Figure 2a). LiTFSI and Li_2S_6 have the highest and lowest $D^{V,b}$ over the whole concentration range, respectively. The transference number of lithium ions in LiTFSI-DOL/DME is significantly higher than those of polysulfide systems and falls in a range of 0.47−0.57. The fraction of current (in the absence of a concentration gradient) carried by Li^+ in Li_2S_6-DOL/DME is in the range of 0.001−0.2, whereas the negative transference numbers clearly distinguish the Li_2S_4-DOL/DME among the three binary systems, i.e., $-0.39 < t_+^{0,b} < -0.32$ (Figure 2b). These small transference numbers impose a very steep gradient of solute concentrations to the polysulfide binary systems under current control and the Li_2S_4 species is clearly the most vulnerable. The ionic conductivity (Figure 2c) of the electrolyte in LiTFSI system is well above 1 mS/cm over the whole concentration range and increases to 14.7 mS/cm at 1 M. The average ionic conductivity in Li_2S_4-DOL/DME and Li_2S_6-DOL/DME systems are less than 20% and 29% of the corresponding value in LiTFSI system, respectively. Table 1 summarizes the measured electrolyte density and partial molar volumes of the solute in the binary and ternary electrolytes.

The thermodynamic factor $\left(1 + \frac{\partial \ln f_{\pm}^{b}}{\partial \ln c^{b}}\right)$ of the three solutes in DOL/DME are presented in Figure 3a. The thermodynamic factor increases with concentration for the three binary systems and significantly deviates from the value expected for an ideal solution (i.e., 1) at lower concentrations. The mean-molar ionic activity coefficients are available by integration of the curves in Figure 3a and with respect to the secondary state of reference. Figure 3b presents these activity coefficients for the three binary systems. The activity coefficients are far from unity for the three electrolyte cases and the highest degree of nonideality belongs to the polysulfide solutions. Higher gradients of potential in these electrolytes are further expected as a direct consequence of their extreme nonideality. Application of the Scatchard's neutral-electrolyte description (i.e., eqs 20−22) to the binary data (i.e., Figure 3b) predicts a similar situation (Figure S1) for the ternary electrolytes of LiTFSI with Li_2S_n (n = 6, 4).

The presence of polysulfides in the ternary electrolytes of LiTFSI is concurrent with a substantial change in the mobility of lithium ions. Figure 4a,b and Figure 4d,e present the transference numbers of lithium ions and polysulfides in the ternary electrolytes of LiTFSI-Li_2S_4-DOL/DME and LiTFSI-Li_2S_6-DOL/DME, respectively. Analogous to the trends found for the binary electrolytes of lithium-polysulfides (Figure 2b), the lithium ions have a higher transference number in the ternary electrolyte of Li_2S_6 (Figure 4d) in comparison to the Li_2S_4 ternary system (Figure 4a). The lithium transference is as low as −0.2 for extremely low concentrations of LITFSI and polysulfide concentrations above 0.1 M. The contribution of polysulfide anions in the ionic current is not negligible (Figure 4b,e) even at very low concentrations of Li_2S_n (n = 4, 6). A better illustration of the polysulfide's detrimental impact on the transference of lithium ions is presented in Figure 4c,f. In these figures, the ratio of ternary and binary transference numbers of lithium ions for the same concentration of LiTFSI is presented for the ternary electrolytes based on Li_2S_4 (Figure 4c) and Li_2S_6 (Figure 4f). Introduction of the Li_2S_n (n = 4, 6) into the binary electrolyte of LiTFSI is concomitant with up to 20% and 80% of reduction in the transference number of lithium ions for polysulfide concentrations as low as 0.01 and 0.1 M, respectively. At lithium salt concentrations below 0.5 M, the onset of polysulfide-induced decline in the cationic transference number of the LiTFSI binary electrolytes stands at a very low concentration of polysulfide species, e.g., 20% decrease in $t^0_{Li^+}$ for a 0.3 M LiTFSI is observed as early as polysulfide concentration exceeds 0.005 M.

The analysis of diffusion in a ternary electrolyte is not trivial since a solute diffuses not only as a response to concentration

DOI: 10.1021/acscentsci.6b00169
ACS Cent. Sci. 2016, 2, 560−568

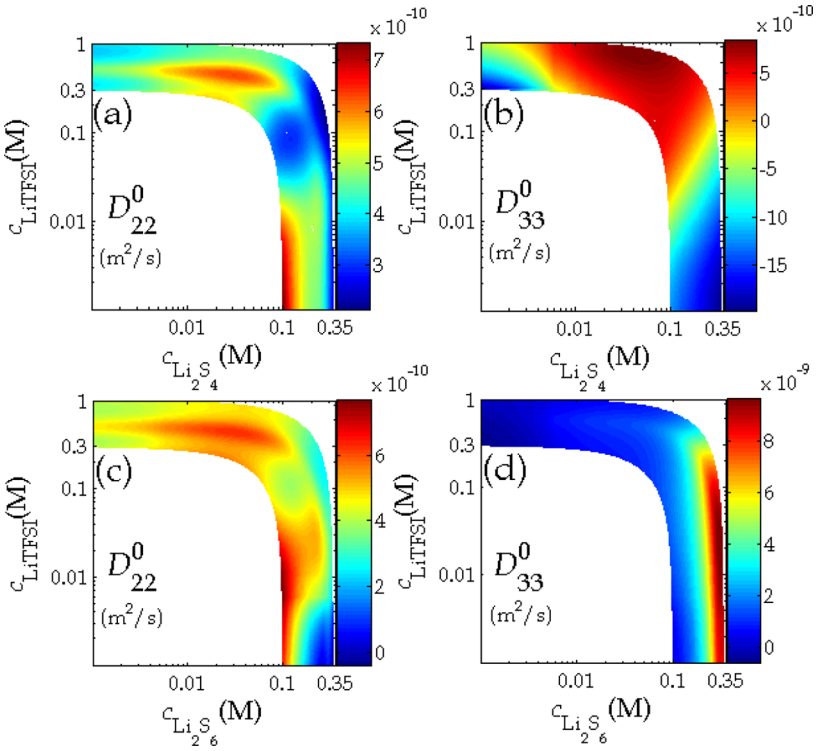

Figure 5. Practical diffusion coefficients of LiTFSI (D^0_{22}) at T = 25 °C in ternary electrolytes of (a) LiTFSI-Li_2S_4 and (c) LiTFSI-Li_2S_6 and those of polysulfides (D^0_{33}) in (b) LiTFSI-Li_2S_4 and (d) LiTFSI-Li_2S_6.

gradient of its own, but also to that of the second solute (eqs 3−5). The practical coefficients characterizing the diffusion rate of LiTFSI and Li_2S_n (n = 4, 6) under their own concentration gradient, i.e., D^0_{22} and D^0_{33}, respectively, are presented in Figure 5. LiTFSI has slightly higher diffusion coefficients (D^0_{22}) in the presence of Li_2S_4 (Figure 5a) rather than Li_2S_6 (Figure 5c). The diffusion behavior (D^0_{33}) of Li_2S_4 and Li_2S_6 in ternary electrolytes of LiTFSI is significantly different. In LiTFSI-Li_2S_6-DOL/DME ternary electrolyte, the diffusion coefficient of Li_2S_6 (D^0_{33} in Figure 5d) is superior to that of LiTFSI (D^0_{22} in Figure 5c), up to 1 order of magnitude. However, the incongruent diffusion of Li_2S_4 (D^0_{33} in Figure 5b) is dominant for polysulfide concentrations lower than 0.01 M and higher than 0.1 M over the full range and c_{LiTFSI} < 0.3 M, respectively.

CONCLUSIONS

Providing D^0_{33} < 0, i.e., incongruent diffusion, the Li_2S_4 species diffuse against their own concentration gradient. This phenomenon is in favor of polysulfide retention at the cathode and against polysulfide crossover toward the lithium anode during cell discharge. The above-mentioned D^0_{33} behavior suggests that the kinetics of Li_2S_6 to Li_2S_4 reduction has a pivotal role in the onset of polysulfide crossover phenomena. A longer residence time of Li_2S_6 at the cathode during cell discharge, i.e., sluggish kinetics of Li_2S_6 reduction, is readily followed by the fast crossover of these species toward the anode. On the contrary, under the fast kinetics of Li_2S_6 reduction, Li_2S_4 species have a very low tendency to shuttle toward the anode during cell discharge. Our diffusion analysis reveals the significant share of Li_2S_6 in the shuttle mechanism and further aging of the lithium−sulfur batteries with a similar electrolyte formulation (i.e., LiTFSI-DOL/DME). The importance of cross-term diffusion coefficients cannot be overlooked. This is clearly evident from the magnitude orders of D^0_{23} and D^0_{32} presented in Figure S2 of Supporting Information. Very high values of D^0_{32} (Figure S2b,d) indicate that a subtle gradient in the concentration of LiTFSI has a significant impact on the diffusion of polysulfide species (i.e., both Li_2S_4 and Li_2S_6). Accordingly, higher rates of cell discharge and charge are counterintuitively in favor of polysulfide retention and crossover, respectively. This might suggest that the relaxation periods after slow rate of discharge and high rate of charge are detrimental to the battery state of health. In contrast to the other two transport properties and not surprisingly, the ionic conductivity of the electrolyte improves upon polysulfide build-up: especially for lower concentrations of LiTFSI (Figure S3).

While it is risky to speculate on the underlying difference in the behavior of the two polysulfides that this analysis clearly points to, we note that under the relatively dilute conditions employed here (<1 M polysulfide) we can expect disproportionation to occur, although it would be less compared to more concentrated solutions. Thus, S_6^{2-} is probably less prone to disproportionation in DOL/DME—generally being subject to cleavage to $S_3^{-\bullet}$ only in EDP solvents[25]—whereas Li_2S_4 is likely to be the end polysulfide that precedes precipitation of Li_2S via disproportionation, as it represents the polysulfide species at the inflection point in a theoretical discharge profile.[20,24−26,45] Computational studies may shed light on the complex dynamics of this system. Further analysis of the system in electron-pair donor (EPD) solvents such as DMSO and DMA where the trisulfide ion dominates the kinetics would be expected to yield very different results, and will be the subject of future studies.

EXPERIMENTAL METHODS

All experiments were conducted at 25 °C inside an argon-filled glovebox with oxygen and water contents below 3 ppm. A VMP3

DOI: 10.1021/acscentsci.6b00169
ACS Cent. Sci. 2016, 2, 560−568

potentiostat was used for the AC-impedance measurements and the galvanostatic polarization studies, together with relaxation tests performed with the aid of a Macpile potentiostat. The density of the electrolytes was measured using an oscillating U-tube digital density meter (DMA 35, Anton-Paar).

To prepare the polysulfides, precise stoichiometric amounts of lithium (as the stabilized powder; FMC Corporation), sulfur, and/or LiTFSI together with the solvent were mixed inside a magnetically stirred glass vial for 4 days. The electrolytes were filtered to remove any leftover reactants.

The 1.27 cm^2 circular lithium electrodes were punched out from a lithium foil with a thickness of 150 μm. All the cells were subjected to three formation cycles after assembly in order to partially stabilize the surface of lithium electrodes. A formation cycle consisted of a charge and discharge segment at 0.05 mA and continued for 0.5 h in each segment. The galvanostatic polarization pulses were 0.1−2 mA in magnitude and continued for 20 min and 10 h in the experiments involved in the measure of the transference number and diffusion coefficient, respectively. Relaxation was recorded until equilibrium was reached both during concentration cell studies and after galvanostatic polarization periods in TP and RD. The AC-impedance spectra were obtained over a frequency range of 200 kHz−50 mHz and with a potential amplitude of 15 mV.

The ionic conductivity of three ternary samples (i.e., (0.2 M LiTFSI, 0.2 M Li_2S_6), (0.4 M TFSI, 0.1 M Li_2S_6), (0.3 M TFSI, 0.2 M Li_2S_6)) were measured in order to check the accuracy of the prediction methodology proposed in this work. The predictions overestimate the experimental data with a maximum error of 20%, which is reasonable considering the experimental protocol.

A representative set of data from the restricted diffusion, transference polarization, and concentration-cell experiments are included in the Supporting Information for the Li_2S_6 electrolytes. Figures S4 and S5 present the data from the TP and RD experiments, respectively, for the binary electrolyte of Li_2S_6 at 0.5M. The results of the concentration-cell experiments are summarized in Figure S6, for the concentration cells at five different concentrations of Li_2S_6, i.e., 0.1, 0.3, 0.5, 0.7, and 1 M.

■ ASSOCIATED CONTENT

Supporting Information

The Supporting Information is available free of charge on the ACS Publications website at DOI: 10.1021/acscentsci.6b00169.

Experimental results and estimations for activity coefficients, cross-term diffusion coefficients, and ionic conductivity of the ternary electrolytes, together with a representative set of raw data for the measurement of binary coefficients (PDF)

■ AUTHOR INFORMATION

Corresponding Author

*E-mail: lfnazar@uwaterloo.ca.

Present Address

†(M.S.) Department of Industrial Engineering, University of Hasselt, Hasselt, Belgium.

Notes

The authors declare no competing financial interest.

■ ACKNOWLEDGMENTS

We gratefully acknowledge the BASF International Scientific Network for Electrochemistry and Batteries for funding. L.F.N. thanks NSERC for a Canada Research Chair, and support via their Discovery Grants program. CYK also thanks the Government of Ontario for Ontario Graduate Scholarship.

■ SYMBOLS AND NOMENCLATURE

ρ	density
c	concentration
$\mathcal{D}$, D	diffusion coefficient
I	binary/ternary fundamental coefficients
L	distance between two electrodes
Φ	potential vs Li
t	transference number and time
ϑ	stochiometric coefficient
F	Faraday constant
z	charge number
π	Pi number
m	slope in transference-polarization experiment
t_p	pulse duration
τ	dimensionless time
I	geometrical-surface current density
κ	ionic conductivity of the electrolyte
y	ionic-strength fraction of the solute in a ternary electrolyte
M	molar mass
N	number of equivalents
$f_{\pm}$	mean-molar ionic activity coefficient
$\bar{V}$	partial molar volume
μ	electrochemical potential

Superscripts

0	solvent-fixed frame (SF)
b	binary electrolyte
V	volume-fixed frame (VF)

Subscripts

a	anion
c	cation
∞	electrolyte bulk at infinite time or distance from the electrode
+	cation in the binary electrolyte
−	anion in the binary electrolyte
0	solvent (i.e., DOL/DME)
1	cation in the ternary electrolyte with common cation (Li^+)
2	anion of the primary solute in the ternary electrolyte with common cation (i.e., $TFSI^-$)
3	anion of the secondary solute in the ternary electrolyte with common cation (i.e., S_6^{-2}/S_4^{-2})
12	first solute in the ternary electrolyte with common cation (i.e., LiTFSI)
13	second solute in the ternary electrolyte with common cation (i.e., Li_2S_6/Li_2S_4)

■ REFERENCES

(1) Evers, S.; Nazar, L. F. New approaches for high energy density lithium-sulfur battery cathodes. *Acc. Chem. Res.* **2013**, *46*, 1135−1141.

(2) Manthiram, A.; Fu, Y.; Chung, S. H.; Zu, C.; Su, Y. S. Rechargeable lithium-sulfur batteries. *Chem. Rev.* **2014**, *114*, 11751−11787.

(3) Erickson, E. M.; Markevich, E. M.; Salitra, G.; Sharon, D.; Hirshberg, D.; de la Llave, E.; Shterenberg, I.; Rozenman, A.; Frimer, A.; Aurbach, D. Development of advanced rechargeable batteries: a continuous challenge in the choice of suitable electrolyte solution. *J. Electrochem. Soc.* **2015**, *162*, A2424−A2438.

(4) Lv, D.; Zheng, J.; Li, Q.; Xie, X.; Ferrara, S.; Nie, Z.; Mehdi, L. B.; Browning, N. D.; Zhang, J. G.; Graff, G. L.; Liu, J.; Xiao, J. High energy density lithium-sulfur batteries: challenges of thick sulfur cathodes. *Adv. Energy Mater.* **2015**, *5*, 1402290−1402298.

(5) Park, K.; Cho, J. H.; Jang, J. H.; Yu, B. C.; de la Hoz, A. T.; Miller, K. M.; Ellison, C. J.; Goodenough, J. B. Trapping lithium polysulfides

DOI: 10.1021/acscentsci.6b00169
ACS Cent. Sci. 2016, 2, 560−568

of a Li-S battery by forming lithium bonds in a polymer matrix. *Energy Environ. Sci.* **2015**, *8*, 2389−2395.
(6) Li, W.; Yao, H.; Yan, K.; Zheng, G.; Liang, Z.; Chiang, Y. M.; Cui, Y. The synergetic effect of lithium polysulfide and lithium nitrate to prevent lithium dendrite growth. *Nat. Commun.* **2015**, *6*, 7436−7443.
(7) Mikhaylik, Y. V.; Akridge, J. R. Polysulfide shuttle study in the Li/S battery system. *J. Electrochem. Soc.* **2004**, *151*, A1969−A1976.
(8) Wild, M.; O'Neill, L. O.; Zhang, T.; Purkayastha, R.; Minton, G.; Marinescu, M.; Offer, G. Lithium sulfur batteries, a mechanistic review. *Energy Environ. Sci.* **2015**, *8*, 3477−3494.
(9) Zhang, S. S.; Read, J. A. A new direction for the performance improvement of rechargeable lithium/sulfur batteries. *J. Power Sources* **2012**, *200*, 77−82.
(10) Manthiram, A.; Chung, S.-H.; Zu, C. Lithium-Sulfur batteries: progress and prospects. *Adv. Mater.* **2015**, *27*, 1980−2006.
(11) Pang, Q.; Liang, X.; Kwok, C. Y.; Nazar, L. F. The importance of chemical interactions between sulfur host materials and lithium polysulfides for advanced lithium-sulfur batteries. *J. Electrochem. Soc.* **2015**, *162*, A2567−A2576.
(12) He, G.; Evers, S.; Liang, X.; Cuisinier, M.; Garsuch, A.; Nazar, L. F. Tailoring porosity in carbon nanospheres for lithium-sulfur battery cathodes. *ACS Nano* **2013**, *7*, 10920−10930.
(13) Elazari, R.; Salitra, G.; Garsuch, A.; Panchenko, A.; Aurbach, D. Sulfur-impregnated activated carbon fiber cloth as a binder-free cathode for rechargeable Li-S batteries. *Adv. Mater.* **2011**, *23*, 5641−5644.
(14) Liang, X.; Garsuch, A.; Nazar, L. F. Sulfur cathodes based on conductive MXene nanosheets for high-performance lithium-sulfur batteries. *Angew. Chem., Int. Ed.* **2015**, *54*, 3907−3911.
(15) Liang, X.; Kwok, C. Y.; Lodi-Marzano, L. M.; Pang, Q.; Cuisinier, M.; Huang, H.; Hart, C. J.; Houtarde, D.; Kaup, K.; Sommer, H.; Brezesinski, T.; Janek, J.; Nazar, L. F. Tuning transition metal oxide-sulfur interactions for long life lithium sulfur batteries: the 'Goldilock' principle. *Adv. Energy Mater.* **2016**, *6*, 150163610.1002/aenm.201501636.
(16) Barghamadi, M.; Best, A. S.; Bhatt, A. I.; Hollenkamp, A. F.; Musameh, M.; Rees, R. J.; Rüther, T. Lithium-sulfur batteries - the solution is in the electrolyte, but is the electrolyte a solution? *Energy Environ. Sci.* **2014**, *7*, 3902−3920.
(17) Xu, R.; Lu, J.; Amine, K. Progress in mechanistic understanding and characterization techniques of Li-S batteries. *Adv. Energy Mater.* **2015**, *5*, 150040810.1002/aenm.201500408.
(18) Lu, Y.-C.; He, Q.; Gasteiger, H. A. Probing the lithium-sulfur redox reactions: A rotating-ring disk electrode study. *J. Phys. Chem. C* **2014**, *118*, 5733−5741.
(19) Barchasz, C.; Molton, F.; Duboc, C.; Lepretre, J. C.; Patoux, S.; Alloin, F. Lithium/sulfur cell discharge mechanism: An original approach for intermediate species identification. *Anal. Chem.* **2012**, *84*, 3973−3980.
(20) Cuisinier, M.; Cabelguen, P.-E.; Evers, S.; He, G.; Kolbeck, M.; Garsuch, A.; Bolin, T.; Balasubramanian, M.; Nazar, L. F. Sulfur speciation in Li-S batteries determined by *operando* X-ray absorption spectroscopy. *J. Phys. Chem. Lett.* **2013**, *4*, 3227−3232.
(21) Gorlin, Y.; Siebel, A.; Piana, M.; Huthwelker, T.; Jha, H.; Monsch, G.; Kraus, F.; Gasteiger, H. A.; Tromp, M. *Operando* characterization of intermediates produced in a lithium-sulfur battery. *J. Electrochem. Soc.* **2015**, *162*, A1146−A1155.
(22) Chivers, T. Ubiquitous trisulfur radical ion $S_3^{-\bullet}$. *Nature* **1974**, *252*, 32−33.
(23) Chivers, T.; Elder, P. J. W. Ubiquitous trisulfur radical anion: fundamentals and applications in materials science, electrochemistry, analytical chemistry and geochemistry. *Chem. Soc. Rev.* **2013**, *42*, 5996−6005.
(24) Cuisinier, M.; Hart, C.; Balasubramanian, M.; Garsuch, A.; Nazar, L. F. Radical or not radical: revisiting lithium-sulfur electrochemistry in non-aqueous electrolytes. *Adv. Energy Mater.* **2015**, *5*, 1401801.
(25) Vijayakumar, M.; Govind, N.; Walter, E.; Burton, S. D.; Shukla, A.; Devaraj, A.; Xiao, J.; Liu, J.; Wang, C.; Karim, A.; Thevuthasan, S. Molecular structure and stability of dissolved lithium polysulfide species. *Phys. Chem. Chem. Phys.* **2014**, *16*, 10923−10932.
(26) Kumaresan, K.; Mikhaylik, Y.; White, R. E. A mathematical model for a lithium-sulfur cell. *J. Electrochem. Soc.* **2008**, *155*, A576−A582.
(27) Hofmann, A. F.; Fronczek, D. N.; Bessler, W. G. Mechanistic modeling of polysulfide shuttle and capacity loss in lithium-sulfur batteries. *J. Power Sources* **2014**, *259*, 300−310.
(28) Albertus, P.; Christensen, J.; Newman, J. Experiments on and modeling of positive electrodes with multiple active materials for lithium-ion batteries. *J. Electrochem. Soc.* **2009**, *156*, A606−A618.
(29) Christensen, J.; Newman, J. A mathematical model for the lithium-ion negative electrode solid electrolyte interphase. *J. Electrochem. Soc.* **2004**, *151*, A1977−A1988.
(30) Christensen, J.; Newman, J. Stress generation and fracture in lithium insertion materials. *J. Solid State Electrochem.* **2006**, *10*, 293−319.
(31) Christensen, J.; Newman, J. Cyclable lithium and capacity loss in Li-ion cells. *J. Electrochem. Soc.* **2005**, *152*, A818−A829.
(32) Zhang, T.; Marinescu, M.; O'Neill, L.; Wild, M.; Offer, G. Modeling the voltage loss mechanisms in lithium-sulfur cells: the importance of electrolyte resistance and precipitation kinetics. *Phys. Chem. Chem. Phys.* **2015**, *17*, 22581−22586.
(33) Marinescu, M.; Zhang, T.; Offer, G. J. A zero dimensional model of lithium-sulfur batteries during charge and discharge. *Phys. Chem. Chem. Phys.* **2016**, *18*, 584−593.
(34) Eroglu, D.; Zavadil, K. R.; Gallagher, K. G. Critical link between materials chemistry and cell-level design for high energy density and low cost lithium-sulfur transportation battery. *J. Electrochem. Soc.* **2015**, *162*, A982−A990.
(35) Ma, Y.; Doyle, M.; Fuller, T. F.; Doef, M. M.; de Jonghe, L. C.; Newman, J. Measurement of a complete set of transport properties for a concentrated solid polymer electrolyte solution. *J. Electrochem. Soc.* **1995**, *142*, 1859−1868.
(36) de Groot, S. R.; Mazur, P. *Non-Equilibrium Thermodynamics*; Dover Publications; New York, 1984.
(37) Miller, D. G. Application of irreversible thermodynamics to electrolyte solutions. I. determination of ionic transport coefficients l_{ij} for isothermal vector transport processes in binary electrolyte systems. *J. Phys. Chem.* **1966**, *70*, 2639−2659.
(38) Miller, D. G. Application of irreversible thermodynamics to electrolyte solutions. II. Ionic coefficients l_{ij} for isothermal vector transport processes in ternary systems. *J. Phys. Chem.* **1967**, *71*, 616−632.
(39) Guggenheim, E. A. *Thermodynamics, An Advanced Treatment for Chemists and Physicists*; Elsevier Science Publishers B. V.; Amsterdam North-Holland, 1967.
(40) Kirkwood, J. G.; Baldwin, R. L.; Dunlop, P. J.; Gosting, L. J.; Kegeles, G. Flow equations and frame of reference for isothermal diffusion in liquids. *J. Chem. Phys.* **1960**, *33*, 1505−1513.
(41) Newman, J.; Thomas-Alyea, K. E. *Electrochemical Systems*; Wiley Interscience; New Jersey, USA, 2004.
(42) Miller, D. G. Activity coefficient derivatives of ternary systems based on Scatchard's neutral electrolyte description. *J. Solution Chem.* **2008**, *37*, 365−375.
(43) Hafezi, H.; Newman, J. Verification and analysis of transference number measurements by the galvanostatic polarization method. *J. Electrochem. Soc.* **2000**, *147*, 3036−3042.
(44) Newman, J.; Chapman, T. W. Restricted diffusion in binary solutions. *AIChE J.* **1973**, *19*, 343−348.
(45) Cuisinier, M.; Cabelguen, P. E.; Adams, B. D.; Garsuch, A.; Balasubramanian, M.; Nazar, L. F. Unique behavior of nonsolvents for polysulfides in lithium-sulfur batteries. *Energy Environ. Sci.* **2014**, *7*, 2697−2705.

DOI: 10.1021/acscentsci.6b00169
ACS Cent. Sci. 2016, 2, 560−568